INSTITUTE OF PHYSICS PUBLISHING JOURNAL OF PHYSICS A: MATHEMATICAL AND GENERAL

J. Phys. A: Math. Gen. **36** (2003) 8373–8392 PII: S0305-4470(03)59386-6

Form factor for a family of quantum graphs: an expansion to third order

Gregory Berkolaiko[1], **Holger Schanz**[2] **and Robert S Whitney**[3]

[1] Department of Mathematics, University of Strathclyde, Glasgow G1 1XH, UK
[2] Max-Planck-Institut für Strömungsforschung und Institut für Nichtlineare Dynamik der Universität Göttingen, Bunsenstraße 10, D-37073 Göttingen, Germany
[3] Theoretical Physics, University of Oxford, 1 Keble Road, Oxford OX1 3NP, UK

Received 7 February 2003, in final form 14 May 2003
Published 23 July 2003
Online at stacks.iop.org/JPhysA/36/8373

Abstract

For certain types of quantum graphs we show that the random matrix form factor can be recovered to at least third order in the scaled time τ from periodic-orbit theory. We consider the contributions from pairs of periodic orbits represented by diagrams with up to two self-intersections connected by up to four arcs and explain why all other diagrams are expected to give higher-order corrections only. For a large family of graphs with ergodic classical dynamics the diagrams that exist in the absence of time-reversal symmetry sum to zero. The mechanism for this cancellation is rather general which suggests that it also applies at higher orders in the expansion. This expectation is in full agreement with the fact that in this case the linear-τ contribution, the diagonal approximation, already reproduces the random matrix form factor for $\tau < 1$. For systems with time-reversal symmetry there are more diagrams which contribute at third order. We sum these contributions for quantum graphs with uniformly hyperbolic dynamics, obtaining $+2\tau^3$, in agreement with random matrix theory. As in the previous calculation of the leading-order correction to the diagonal approximation we find that the third-order contribution can be attributed to exceptional orbits representing the intersection of diagram classes.

PACS numbers: 03.65.N, 05.45.Mt

1. Introduction

The recent work of Sieber and Richter [1, 2] has renewed the hope that spectral correlations in systems with chaotic classical analogue can be explained within periodic-orbit theory. The universality of these correlations, known as the BGS conjecture [3], is supported by overwhelming numerical evidence [4]. On the other hand there is no satisfactory theory for individual chaotic systems, i.e. without any disorder averages. Numerically it was found that on time scales longer than the ergodic time of the classical analogue, the fluctuations in the

energy spectrum of a quantum system follow those of an appropriate ensemble of random matrices. For random matrices, the form factor $K(\tau)$, which is the Fourier transform of the spectral two-point correlator, is

$$\begin{aligned} K_{\mathrm{GOE}}(\tau) &= 2\tau - \tau\log(1+2\tau) \qquad (0 \leqslant \tau \leqslant 1) \\ &= 2\tau - 2\tau^2 + 2\tau^3 + O(\tau^4) \end{aligned} \tag{1}$$

for systems with time-reversal symmetry (TR), or

$$K_{\mathrm{GUE}}(\tau) = \tau \qquad (0 \leqslant \tau \leqslant 1) \tag{2}$$

for systems with no time-reversal symmetry (NTR) [5].

The semiclassical limit of the form factor in a quantum chaotic system can be written in terms of a double sum over periodic orbits (PO) using the Gutzwiller trace-formula [6]. On short times the relatively small number of contributing periodic orbits allows explicit calculation, however the number of POs proliferates exponentially with time, so evaluating the sum exactly quickly becomes impossible. In any case the universality of the BGS conjecture suggests that beyond the ergodic time the form factor does not depend on the specific dynamics of the given system. Berry [7] explained that this universality arises from the combined contributions of the huge number of ergodic POs. He then calculated the form factor, neglecting all correlations between POs other than exact symmetries. Within this 'diagonal approximation', he obtained the leading order in τ of the random matrix theory (RMT) result. Efforts to reproduce equations (1), (2) beyond the diagonal approximation have been limited in their success. At present there is no way to derive the series expansion of equation (1) from the POs of any chaotic system, nor is there a good explanation of why equation (2) happens to be exactly reproduced by the diagonal approximation for $\tau \leqslant 1$.

Currently we only know how to go beyond the diagonal approximation in a few special cases. In [1, 2] it was shown, that for uniformly hyperbolic and time-reversal invariant billiards on surfaces with constant negative curvature the second-order contribution $-2\tau^2$ is related to correlations within pairs of orbits differing in the orientation of one of the two loops resulting from a self-intersection of the orbit. We went on to derive the same result for a large family of quantum graphs [8, 9] with ergodic classical dynamics, in particular our result was *not* restricted to uniformly hyperbolic dynamics [10]. A subsequent study [11] indicated that the mechanism generating the contribution $-2\tau^2$ also works for systems with antiunitary symmetries other than simple time reversal.

Given these results it is a plausible conjecture that in analogy with disordered systems [12] the terms in the power series expansion of $K(\tau)$ can be identified with the contributions of orbit pairs generated by more and more self-intersections. In the present paper we will explore this idea for a particular model system: extending our recent paper [10] we will calculate the form factor up to order τ^3 for a particular family quantum graphs.

This paper is organized as follows: In section 2, we define our model and explain how the form factor can be expressed as a double sum over periodic orbits. In section 3, this sum is rewritten in terms of diagrams, representing all orbits with a given number and topology of self-intersections. Diagrams resulting in a contribution of order τ^3 are considered explicitly. In section 4, we show that those diagrams which do not require time-reversal invariance cancel each other. The summation over the additional diagrams in graphs with time-reversal invariance is performed in section 5, unfortunately here our results are limited to a family of graphs with uniformly hyperbolic classical dynamics. Finally, in section 6 we explain how we selected the diagrams which give τ^3-contributions by establishing a heuristic rule which predicts the order of a given diagram's contribution without an explicit calculation.

2. Quantum graphs and periodic-orbit theory

We consider graphs with N vertices connected by a total of B directed bonds. A bond leading from vertex m to vertex l is denoted by (m, l). For graphs with time-reversal invariance it is necessary that for any bond (m, l) there exists also the reversed bond (l, m). We do not rule out the possibility of loops, i.e. bonds of the form (m, m).

The discrete quantum dynamics on a graph are defined in terms of a $B \times B$ unitary time-evolution operator $S^{(B)}$, which has matrix elements $S^{(B)}_{m'l',lm}$ describing the transition amplitudes from the directed bond (m, l) to (l', m').[4] The topology of the underlying graph is reflected in the quantum dynamics because the amplitudes are non-zero only if the two bonds are connected at a vertex, $l = l'$. We choose

$$S^{(B)}_{m'l',lm} = \delta_{l'l}\sigma^{(l)}_{m'm}\,\mathrm{e}^{\mathrm{i}\phi_{ml}} \tag{3}$$

with $\sigma^{(l)}_{m'm}$ denoting the *vertex-scattering matrix* at vertex l. An explicit example of such a graph will be given in section 5, here we keep the discussion as general as possible. The phases ϕ_{ml} are random variables distributed uniformly in $[0, 2\pi]$ and define for fixed B an ensemble of matrices $S^{(B)}$ which can be used for averaging. It is possible to interpret this ensemble as an infinite energy average for a given quantum graph with rationally independent bond lengths [8]. For a unitary operator such as $S^{(B)}$ the form factor is defined at integer times $t = 0, 1, \ldots$, by

$$K^{(B)}(\tau) = B^{-1}\langle|\mathrm{Tr}\, S^t|^2\rangle_{\{\phi\}} \tag{4}$$

where τ is the scaled time $\tau = t/B$. See [4] for more details on the description of two-point correlations for unitary operators. For finite B, the form factor (4) should be compared to ensembles of unitary random matrices of dimension B (CUE for NTR, COE for TR). However, we are interested here in the limit of large graphs $B \to \infty$, keeping the scaled time τ fixed

$$K(\tau) = \lim_{B\to\infty} K^{(B)}(\tau) \tag{5}$$

because this is equivalent to the semiclassical limit of chaotic systems [8]. It is in this limit that the form factor is expected to assume the corresponding universal form (1) or (2).

Associated with the unitary matrix S is the doubly stochastic matrix M with

$$M^{(B)}_{m'l,lm} = \left|S^{(B)}_{m'l,lm}\right|^2 = \left|\sigma^{(l)}_{m'm}\right|^2. \tag{6}$$

It defines a Markov chain on the graph which represents the classical analogue of our quantum system [8, 13]. The matrix M can be considered as the Frobenius–Perron operator of the discrete classical dynamics. Matrix elements of powers of this operator give the classical probability to get from bond (m, l) to bond (k, n) in t steps

$$P^{(t)}_{(m,l)\to(k,n)} = [M^t]_{nk,lm}. \tag{7}$$

Under very general conditions it can be shown that the dynamics generated by M is ergodic and mixing[5], i.e. for fixed B and $t \to \infty$ all transition probabilities become equal

$$P^{(t)}_{(m,l)\to(k,n)} \to B^{-1} \qquad \text{as} \quad t \to \infty \qquad \forall(m, l), (k, n). \tag{8}$$

However, since in equation (5) the limits $B \to \infty$ and $t \to \infty$ are connected by fixing τ, equation (8) is not sufficient for showing agreement between PO expansion and RMT. We need a stronger condition such as

$$P^{(\tau B)}_{(m,l)\to(k,n)} \to B^{-1} \qquad \text{as} \quad B \to \infty \qquad \forall(m, l), (k, n). \tag{9}$$

[4] We drop the parentheses when a bond is used as an index of a matrix.

[5] It is plausible to assume that these conditions are satisfied if the underlying graph is connected and one excludes special cases such as bipartite graphs [14].

This was already discussed in [15] in connection with the diagonal approximation. In fact the precise condition may in principle depend on the order to which agreement with RMT is required. In [10] we derived a condition sufficient for the leading-order correction to the diagonal approximation which was slightly stronger than equation (9): the speed of convergence to equidistribution with increasing B cannot be arbitrarily slow. However, exponential convergence (corresponding to a spectral gap of M which is bounded away from zero uniformly in B) is sufficient in any case. We will restrict ourselves to graphs which obey this condition rather than derive a more precise condition for the applicability of equation (9) to the summation of third-order diagrams.

A connection between the quantum form factor equation (4) and the classical dynamics given by equation (6) can be established by representing the form factor as a sum over (classical) POs. We expand the matrix powers of S in equation (4) and obtain sums over products of matrix elements $S_{p_2p_1,p_1p_t}\cdots S_{p_4p_3,p_3p_2}S_{p_3p_2,p_2p_1}$. Obviously each such product can be specified by a sequence of t vertices. Vertex sequences which are identical up to a cyclic shift give identical contributions and will be combined into the contribution of a periodic orbit $P = [p_1, \ldots, p_t]$. For most POs there are t different cyclic shifts. Exceptions to this rule are possible if a PO is a repetition of a shorter orbit, but the fraction of such orbits decreases exponentially in t. Moreover, if we assume the existence of the limit (5), we can approach it through sequences of prime t, which totally excludes repetitions. We obtain

$$\operatorname{Tr} S^t = t \sum_P A_P \, \mathrm{e}^{\mathrm{i}\phi_P} \tag{10}$$

with $A_P = \prod_{i=1}^t \sigma^{(p_i)}_{p_{i+1},p_{i-1}}$ and $\phi_P = \sum_{i=1}^t \phi_{p_{i+1},p_i}$ (vertex indices are taken modulo t). Substituting this into equation (4) we obtain a double sum over periodic orbits

$$K^{(B)}(\tau) = \frac{t^2}{B} \left\langle \sum_{P,Q} A_P A_Q^* \, \mathrm{e}^{\mathrm{i}(\phi_P - \phi_Q)} \right\rangle_{\{\phi\}} . \tag{11}$$

We can now perform the average over the phases ϕ_{ml} associated with the directed bonds. If the system does not have time-reversal symmetry, all bond phases can be varied independently. The total phase of an orbit, ϕ_P, can be written as linear combinations of the bond phases, $\phi_P = \sum_{lm} n^{(P)}_{lm} \phi_{lm}$, where $n^{(P)}_{lm}$ counts visits of the orbit P to bond (m, l). Then we can average over ϕ_{lm} using

$$\left\langle \mathrm{e}^{\mathrm{i}(n^{(P)}_{lm}\phi_{lm} - n^{(Q)}_{lm}\phi_{lm})} \right\rangle_{\phi_{lm}} = \delta_{n^{(P)}_{lm}, n^{(Q)}_{lm}} . \tag{12}$$

Thus averaging over all bond phases, $\{\phi\}$, amounts to picking out only those pairs of orbits which visit the same set of bonds the same number of times. Therefore, the form factor for a quantum graph with no time-reversal symmetry (NTR) is

$$K^{(B)}_{\mathrm{NTR}}(\tau) = \frac{t^2}{B} \sum_{P,Q} A_P A_Q^* \left[\prod_{lm} \delta_{n^{(P)}_{lm}, n^{(Q)}_{lm}} \right] . \tag{13}$$

Time-reversal symmetry implies symmetric vertex-scattering matrices

$$\sigma^{(l)}_{m'm} = \sigma^{(l)}_{mm'} \tag{14}$$

and that the phases of a pair of bonds (m, l) and (l, m) related by time reversal obey $\phi_{ml} = \phi_{lm}$. The average in equation (11) runs over all independent phases and results in

$$\langle \mathrm{e}^{\mathrm{i}(\phi_P - \phi_Q)} \rangle_{\{\phi\}} = \prod_{l \geqslant m} \delta_{n^{(P)}_{lm} + n^{(P)}_{ml}, n^{(Q)}_{lm} + n^{(Q)}_{ml}} . \tag{15}$$

Thus averaging over all independent bond phases, $\{\phi\}$, amounts in this case to picking out only those pairs of orbits which visit the same set of bonds, or their time reverses, the same number of times. Hence, the form factor for a quantum graph with time-reversal symmetry is

$$K_{\mathrm{TR}}^{(B)}(\tau) = \frac{t^2}{B}\sum_{P,Q} A_P A_Q^* \left[\prod_{l\geqslant m} \delta_{n_{lm}^{(P)}+n_{ml}^{(P)},\, n_{lm}^{(Q)}+n_{ml}^{(Q)}}\right]. \tag{16}$$

If the graph is defined to have bonds with fixed lengths and magnetic vector potential as in [8], we can average over an infinite energy window (for NTR systems we also average over the vector potential). Then the orbit pairs contributing to the form factor are those where P, Q have exactly the same lengths. On a graph with rationally independent bond lengths this is equivalent to

$$\mathrm{NTR}: \quad n_{lm}^{(P)} = n_{lm}^{(Q)} \qquad \forall l, m \tag{17}$$

$$\mathrm{TR}: \quad n_{lm}^{(P)} + n_{ml}^{(P)} = n_{lm}^{(Q)} + n_{ml}^{(Q)} \qquad \forall l, m \tag{18}$$

so this averaging procedure also leads to equations (13) and (16).

3. The expansion in self-intersections of the periodic orbits

3.1. From orbits to diagrams

The calculation of the form factor is now reduced to a combinatorial problem: the sum over the pairs P, Q in equations (13) and (16) must be organized such that equation (17) or (18) is satisfied. This can be done by composing P and Q from the same segments, or *arcs*, which appear in P and Q in different order and/or orientation. This is possible if the orbit P contains self-intersections, i.e. vertices which are traversed more than once, see figure 1 for examples. In general, an orbit P has many self-intersections and many partner orbits Q satisfying equations (17), (18) such that a summation over all possible Q for a fixed P is too complicated. Instead we fix a permutation of arcs followed by the time reversal of selected arcs and sum first over all possible pairs of orbits P, Q related by this transformation. The clearest way to represent all possible transformations is graphical (figure 1), hence we refer to them as diagrams. The sum over all diagrams finally gives the form factor.

The main problem with this approach is to ensure that each orbit pair P, Q is counted once and only once. This is difficult because for some pairs P, Q the operation transforming P into Q is not unique. Such orbit pairs are relatively rare in number but nevertheless they give essential contributions to the form factor [10]. We will explain our techniques for preventing the double counting of orbit pairs in sections 3.2 and 3.3.

If we consider P as a single arc with no intersections, $Q = P$ is the only possibility in the NTR case. For TR the orientation of the arc can be reversed such that $Q = \overline{P}$ is a second option. The corresponding diagrams have a simple circular shape. Summation over these orbit pairs is nothing other than the diagonal approximation. It produces $K_{\mathrm{NTR1}} = \tau$ and $K_{\mathrm{TR1}} = 2\tau$, respectively. In [10] we considered orbits, P, made from two arcs, 1 and 2, joined at a single intersection α and evaluated the (off-diagonal) contribution corresponding to the resulting 8-shaped diagram. We found this gave rise to the second-order term in equation (1), $K_{\mathrm{TR2}} = -2\tau^2$, while there is no contribution of this order for a NTR system. In this paper, we calculate the τ^3-contribution by assuming that P contains three or four arcs connected at intersections. A discussion of why only these particular diagrams contribute to the τ^3-contribution is deferred to section 6.

NTR3a
orbits : $1\alpha 2\beta 3\alpha 4\beta$ and $1\alpha 4\beta 3\alpha 2\beta$
factors : $1/4$
restrictions : $(1-\delta_{s_2 s_4})\ (1-\delta_{s_1 s_3})$

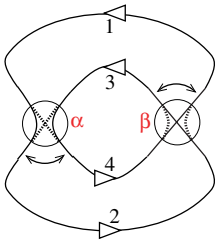

NTR3b
orbits : $1\alpha 2\alpha 3\alpha$ and $1\alpha 3\alpha 2\alpha$
factors : $1/3$
restrictions : $(1-\delta_{s_1 s_2})\ (1-\delta_{s_1 s_3})\ (1-\delta_{s_2 s_3})$

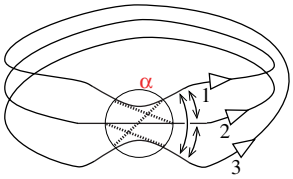

TR3a
orbits : $1\alpha 2\beta 3\alpha 4\beta$ and $1\alpha 4\beta \overline{2}\alpha \overline{3}\beta$
factors : $1/2$
restrictions : $(1-\delta_{s_2 s_4})\ (1-\delta_{s_3 s_4})$
with $1 \neq \overline{2}$ and $1 \neq 3$

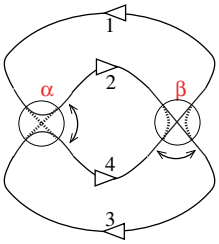

TR3b
orbits : $1\alpha 2\beta 3\beta 4\alpha$ and $1\alpha \overline{4}\beta 3\beta \overline{2}\alpha$
factors : $1/2$
restrictions : $(1-\delta_{s_2 f_4})\ (1-\delta_{s_4 f_2})$
with $1 \neq \overline{1}$ and $3 \neq \overline{3}$

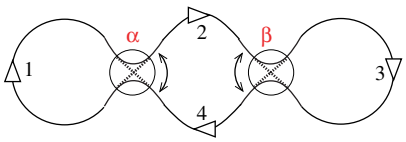

TR3c
orbits : $1\alpha 2\alpha 3\alpha$ and $1\alpha 3\alpha \overline{2}\alpha$
factors : 1
restrictions : $(1-\delta_{s_2 s_3})\ (1-\frac{1}{2}\,\delta_{s_2 f_3})\ (1-\frac{1}{2}\,\delta_{s_1 f_2})$
with $1 \neq \overline{1}$, $2 \neq \overline{2}$ and $3 \neq \overline{3}$

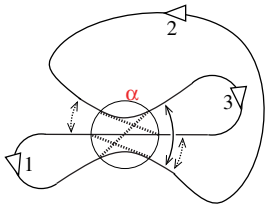

Figure 1. Topology of NTR3a, NTR3b, TR3a, TR3b and TR3c. In each case a pair of orbits is shown. One follows the solid line throughout (in the direction marked by triangular arrows). The second follows the solid lines (possibly with reversed direction) except at the intersections (denoted by circles) where it follows the dotted line. Each circle represents a single vertex where a self-intersection of the orbit occurs. Next to each topology we give the corresponding weight factor (section 3.2) and the restrictions (section 3.3). Restrictions are indicated by the double-headed arrows. Solid arrows indicate a 'full' restriction of the form $(1-\delta_{ij})$, while dotted arrows indicate a 'half' restriction of the form $(1-\frac{1}{2}\delta_{ij})$.

We begin by listing in figure 1 all diagrams which contribute at third order in τ. We denote arcs by numbers $1, 2, \ldots$, and the intersection points by Greek letters $\alpha, \beta, \ldots$. An arc can be identified by a sequence of vertices, which does not include the intersection vertices, or, alternatively, by a sequence of bonds, which includes the bonds from and to the intersection

points. The length of the ith arc is denoted by t_i and is defined as the number of bonds in the arc (which is one more than the number of vertices in the arc). The sum of the lengths of all arcs gives t, the length of the orbit. The length of an arc is at least one. For an arc i leading from α to β we denote the first vertex following α by s_i and the last vertex before β by f_i. In the degenerate case when the arc going from α to β is the single bond (α, β) and does not contain any vertices ($t_i = 1$) this implies $s_i = \beta$ and $f_i = \alpha$.

As shown in figure 1, the arcs forming an orbit P and its partner Q are identical, but the way they are connected at the intersections differs. The orbit P is given by the connections drawn as continuous lines, while its partner orbit Q is given by connections drawn as dotted lines. The orbits P and Q are also written as a symbolic code to the left of each diagram: a path that goes from the beginning of arc 1 to vertex α then on arc 2 to vertex β and so on is denoted as $1\alpha 2\beta\cdots$. The diagrams in figure 1 divide into two classes, NTR and TR. In the NTR diagrams all the arcs of Q have the same orientation as the corresponding arcs in P, while in the TR diagrams some of the arcs of Q are time reversed. For a system with no time-reversal symmetry, only the two NTR diagrams are possible, thus there are two τ^3-contributions to the form factor,

$$K_{\mathrm{NTR3}} = K_{\mathrm{NTR3a}} + K_{\mathrm{NTR3b}}. \tag{19}$$

For a system with time-reversal symmetry, diagrams in both classes contribute and the form factor is a sum of five terms

$$K_{\mathrm{TR3}} = 2\left(K_{\mathrm{NTR3a}} + K_{\mathrm{NTR3b}} + K_{\mathrm{TR3a}} + K_{\mathrm{TR3b}} + K_{\mathrm{TR3c}}\right). \tag{20}$$

The factor of two is due to the fact that for every diagram in figure 1 there is another one with Q replaced by its complete time reversal, $\overline{Q}$, which gives an identical contribution.

3.2. Avoiding double counting I: multiplicity factors

The set of diagrams possesses certain degeneracies which can be accounted for by simple prefactors multiplying the contributions. One such degeneracy is taken care of by the factor of two in equation (20). In this subsection we discuss how to determine the other multiplicity factors arising due to the cyclicity of the POs and symmetries in the diagrams. To sum over all orbit pairs P, Q for a given diagram we sum over all possible arcs forming the orbit P. Consider the diagram NTR3a as an example. Let l_1 and l_3 be some fixed arcs starting at β and ending at α, while l_2 and l_4 denote arcs from α to β. As we sum over all possible realizations of arcs 1, 2, 3, 4 in NTR3a, we encounter a particular orbit P where these arcs are given by

$$1 = l_1 \qquad 2 = l_2 \qquad 3 = l_3 \qquad 4 = l_4. \tag{21}$$

However, we also encounter the orbit P' where the arcs are

$$1 = l_3 \qquad 2 = l_4 \qquad 3 = l_1 \qquad 4 = l_2. \tag{22}$$

The orbit P' is related to P by a cyclic shift and, therefore, it is actually the same orbit. As we are focusing on *pairs* of orbits, we check the partner orbits resulting from P and P', too. The partners for P and P' are $Q = [l_1, \alpha, l_4, \beta, l_3, \alpha, l_2, \beta]$ and $Q' = [l_3, \alpha, l_2, \beta, l_1, \alpha, l_4, \beta]$, respectively, and they are also related by a cyclic shift. Hence in the process of summation we will encounter the same orbit pair four times, once for each of the four possible cyclic permutations of P. To compensate for this we introduce a multiplicity factor of a quarter.

To put this formally, we denote by $q(P)$ the operation transforming P into Q for a given diagram, e.g., $q_{\mathrm{NTR3a}}([1234]) = [1432]$ and $q_{\mathrm{TR3a}}([1234]) = [14\bar{2}\bar{3}]$. Further we denote by σ the (cyclic) left shift of the symbolic code, i.e. $\sigma([1234]) = [2341]$. To determine the multiplicity factor we need to count all cyclic permutations σ^k such that

$$q \circ \sigma^k(P) = \sigma^{k'} \circ q(P) \qquad \text{or} \qquad q \circ \sigma^k(P) = \sigma^{k'} \circ \overline{q(P)} \tag{23}$$

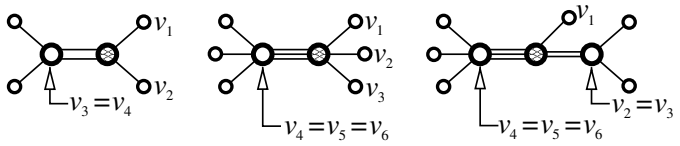

Figure 2. Examples of ambiguous intersections, where we have removed the ambiguity by placing the intersection (the shaded vertex) as far to the right as possible. This is enforced in the left-hand diagram by introducing a factor of $(1-\delta_{v_1v_2})$, while in the other diagrams it is enforced by a factor of $(1-\delta_{v_1v_2}\delta_{v_1v_3})$.

for some k' and arbitrary P, i.e. application of q to the shifted code yields the same or the completely time-reversed result, up to another shift. Obviously the second option is only applicable to the TR diagrams. Noting that the trivial solution $k=k'=0$ is always available, we proceed to list the factors for each diagram.

- NTR3a: We have $q_{\mathrm{NTR3a}}\circ\sigma^k=\sigma^{4-k}\circ q_{\mathrm{NTR3a}}$ for any $k=0,1,2,3$ and consequently $m_{\mathrm{NTR3a}}=4$.
- NTR3b: Similarly we have $q_{\mathrm{NTR3b}}\circ\sigma^k=\sigma^{3-k}\circ q_{\mathrm{NTR3b}}$ for $k=0,1,2$ and $m_{\mathrm{NTR3b}}=3$.
- TR3a: The only nontrivial solution to equation (23) is $k=2$ where $q_{\mathrm{TR3a}}\circ\sigma^2=\overline{q_{\mathrm{TR3a}}}$. Therefore we have $m_{\mathrm{TR3a}}=2$.
- TR3b: The only nontrivial solution is $k=2$ where $q_{\mathrm{TR3b}}\circ\sigma^2=\sigma^2\circ q_{\mathrm{TR3b}}$. Therefore we have $m_{\mathrm{TR3b}}=2$.
- TR3c: Equation (23) has no solution besides the identity $k=0$, therefore $m_{\mathrm{TR3c}}=1$.

When we evaluate the contribution from each diagram we will include a factor $1/m$ in order to compensate for the ambiguity just described.

3.3. Avoiding double counting II: restrictions and exceptions

As shown in [10], *tangential* self-intersections of orbits are a potential source for double counting of orbits which must carefully be avoided. By a *tangential* intersection we mean the situation where an orbit does not merely cross itself but follows itself for at least one bond. For example, the orbit

$$\cdots\to f_i\to\alpha\to\beta\to s_{i+1}\to\cdots\to f_{j+1}\to\beta\to\alpha\to s_{j+1}\to\cdots \qquad (24)$$

crosses itself along the non-directed bond (α,β). It is easy to mistakenly count such an orbit once with α as the intersection point and once with β as the intersection point. We avoid this using a method outlined in [10]. We uniquely define the intersection point by ruling that if there is an ambiguity then the intersection is as far to one side as possible. As an example we show some ambiguous intersections in figure 2 and insist that the intersection is as far to the right as possible. For the 2-intersection we do this by demanding that $v_1\neq v_2$, this is achieved by introducing a factor of the type $\left(1-\delta_{v_1v_2}\right)$, referred to as a *restriction* on the diagram. For the 3-intersections a restriction of the form $\left(1-\delta_{v_1v_2}\delta_{v_1v_3}\right)$ removes the ambiguity. However, we will not actually use this restriction on any 3-intersection, because we will see that *stronger* restrictions apply in the diagrams we evaluate.

For NTR3a, TR3a and TR3b we choose the following restrictions to ensure that the ambiguities at intersections are removed

- NTR3a: $\Delta_{\mathrm{NTR3a}}=\left(1-\delta_{s_2s_4}\right)\left(1-\delta_{s_1s_3}\right)$
- TR3a: $\Delta_{\mathrm{TR3a}}=\left(1-\delta_{s_2s_4}\right)\left(1-\delta_{s_3f_4}\right)$
- TR3b: $\Delta_{\mathrm{TR3b}}=\left(1-\delta_{s_2f_4}\right)\left(1-\delta_{s_4f_2}\right)$

where s_i denotes the first vertex on the arc i and f_i denotes the last. We wish to emphasize that there is no unique way of imposing the restrictions, since they are merely convenient ways of excluding the double counting of certain contributions. What is more, the individual results for NTR3a, NTR3b, TR3a, TR3b and TR3c may depend on the particular choice of restrictions. Only the final sums in equations (19) and (20) do not depend on them.

Now that we come to NTR3b, we will see exactly how much freedom we have in choosing restrictions. First we want to ensure that we count tangential intersections correctly. For a 3-intersection, such as the one in NTR3b, we could do this by setting $\Delta_{\mathrm{NTR3b}} = \left(1-\delta_{s_1 s_2}\delta_{s_2 s_3}\right)$. However we also note that there are ambiguous contributions which could be counted in either NTR3a or NTR3b:[6]

- NTR3b with either $s_1 = s_2$, $s_2 = s_3$ or $s_1 = s_3$ is equivalent to NTR3a with any of the following: $(t_1 = 1\ \&\ f_1 = f_3)$, $(t_2 = 1\ \&\ f_2 = f_4)$, $(t_3 = 1\ \&\ f_1 = f_3)$ or $(t_4 = 1\ \&\ f_2 = f_4)$
- NTR3b with either $f_1 = f_2$, $f_2 = f_3$ or $f_1 = f_3$ is equivalent to NTR3a with any of the following: $(t_1 = 1\ \&\ s_1 = s_3)$, $(t_2 = 1\ \&\ s_2 = s_4)$, $(t_3 = 1\ \&\ s_1 = s_3)$ or $(t_4 = 1\ \&\ s_2 = s_4)$.

Obviously we should only count each of these contributions once, but we have the freedom to choose whether we count each of them in NTR3a or NTR3b. The physical quantities (19) and (20) contain the sum of NTR3a and NTR3b, so all choices are strictly equivalent. However given that we have imposed the restriction $s_1 \neq s_3$ on NTR3a the second type of orbits (NTR3b with $f_i = f_j$) cannot belong to NTR3a. Thus, once we have chosen the above restrictions for NTR3a we are forced into the choice

$$\Delta_{\mathrm{NTR3b}} = \left(1-\delta_{s_1 s_2}\right)\left(1-\delta_{s_1 s_3}\right)\left(1-\delta_{s_2 s_3}\right). \tag{25}$$

Before we can move on to TR3c, we must first look carefully at the restriction we placed on TR3a. In section 3.2 we introduced the factor of $1/2$ to avoid double counting. The double counting in this particular instance was caused by the permutation $\sigma^2 = [3412]$ which swaps around arcs $1 \leftrightarrow 3$ and $2 \leftrightarrow 4$ and produces a pair $P' = \sigma^2(P)$ and $Q' = \sigma^2(Q)$, which is identical to P, Q up to a shift. However, the restriction $s_2 \neq f_4$ that we introduced on TR3a is *not* symmetric with respect to this permutation. For the orbits satisfying $s_1 \neq f_2$ and $s_3 \neq f_4$ this does not present any problems. Let us consider what happens when arcs 1 and 2 are different but have $s_1 = f_2$. This orbit is still counted twice in the summation over all possible arcs, but in the second instance the intersection point β is shifted, resulting in $t_1' = t_3 + 1, t_2' = t_4 + 1, t_3' = t_1 - 1, t_4' = t_2 - 1$. We illustrate that by the following example of orbits which contribute to TR3a. The pair

$$P = [\beta, \gamma, a, \alpha, b, \gamma, \beta, d, \alpha, c] \qquad \text{and} \qquad Q = [\beta, \gamma, a, \alpha, c, \beta, \gamma, b, \alpha, d] \tag{26}$$

is obtained by combining the arcs

$$\text{arc } 1 = (\beta, \gamma) \to (\gamma, a) \to (a, \alpha) \qquad \text{arc } 3 = (\beta, d) \to (d, \alpha) \tag{27}$$

$$\text{arc } 2 = (\alpha, b) \to (b, \gamma) \to (\gamma, \beta) \qquad \text{arc } 4 = (\alpha, c) \to (c, \beta) \tag{28}$$

with the intersection points α and β, or by combining the arcs

$$\text{arc } 1 = (\gamma, \beta) \to (\beta, d) \to (d, \alpha) \qquad \text{arc } 3 = (\gamma, a) \to (a, \alpha) \tag{29}$$

$$\text{arc } 2 = (\alpha, c) \to (c, \beta) \to (\beta, \gamma) \qquad \text{arc } 4 = (\alpha, b) \to (b, \gamma) \tag{30}$$

[6] This abundance of choice, when any of the three NTR3b diagrams is equivalent to any of the four NTR3a diagrams is another manifestation of the cyclic symmetry discussed in section 3.2 and is taken care of by the multiplicity factors.

with the intersection points α and γ. We therefore see that the factor of $1/2$ works also when $s_1 = f_2$. But not when, in addition to $s_1 = f_2$, t_1 or t_2 is equal to 1. These orbits appear in the sum for TR3a only once and are subsequently multiplied by $1/2$, so it appears we miscount their contribution. On the other hand these orbits can also be counted in TR3c, as shown below. We find it convenient to keep the above restriction on TR3a, thus counting half their contribution in TR3a. This forces us to count the other half of their contribution in TR3c.

Now we can move on to finding the restrictions on TR3c. First we list the special cases of TR3c which could be counted in other diagrams.

(i) TR3c with $s_1 = f_2$ is equiv. to TR3a with ($t_3 = 1$ & $s_3 = f_4$) or ($t_1 = 1$ & $s_1 = f_2$)
(ii) TR3c with $s_2 = f_3$ is equiv. to TR3a with ($t_4 = 1$ & $s_3 = f_4$) or ($t_2 = 1$ & $s_1 = f_2$)
(iii) TR3c with $s_2 = s_3$ is equiv. to TR3a with ($t_1 = 1$ & $f_1 = f_3$) or ($t_3 = 1$ & $f_1 = f_3$)
(iv) TR3c with $f_1 = f_2$ is equiv. to TR3a with ($t_2 = 1$ & $s_2 = s_4$) or ($t_4 = 1$ & $s_2 = s_4$)
(v) TR3c with $s_1 = f_1$ is equiv. to TR3b with ($t_2 = 1$ & $s_2 = f_4$) or ($t_4 = 1$ & $s_4 = f_2$)
(vi) TR3c with $s_3 = f_3$ is equiv. to TR3b with ($t_2 = 1$ & $s_2 = f_4$) or ($t_4 = 1$ & $s_4 = f_2$)

Now we carefully count in TR3c only those contributions which have not already been counted in TR3a or TR3b. Lines (i) and (ii) above show that cases $s_1 = f_2$ and $s_2 = f_3$ should be counted in TR3c with the factor $1/2$. Line (iii) shows that the case $s_2 = s_3$ should not be counted in TR3c as it is fully counted in TR3a; the case $f_1 = f_2$, line (iv), should be fully counted in TR3c. Lines (v) and (vi) show that the cases $s_1 = f_1$ and $s_3 = f_3$ are not counted in TR3b and should be fully counted in TR3c. All this is realized by the restrictions

$$\Delta_{\mathrm{TR3c}} = \left(1 - \delta_{s_2 s_3}\right)\left(1 - \tfrac{1}{2}\delta_{s_2 f_3}\right)\left(1 - \tfrac{1}{2}\delta_{s_1 f_2}\right). \tag{31}$$

Above we have ensured that no orbits are double counted among the diagrams NTR3a, NTR3b, TR3a, TR3b and TR3c. However, we should also exclude the orbits that have already been counted at lower orders of the expansion. Considering NTR3a, if arc 1 is identical to arc 3 (or arc 2 identical to arc 4), the diagram is reduced to giving a contribution to the diagonal approximation, so it should not be counted here. Fortunately, the restrictions we have put on NTR3a ensure that this contribution is not counted. Moving on to NTR3b, if any two arcs in the NTR3b diagram are self-retracing the diagram reduces to a diagram already counted as a τ^2-contribution in a TR system. Therefore, in the TR case, we should subtract its contribution from the sum. However, we will see at the end of section 4.1 that such a contribution is zero.

For TR3a, we insist that $1 \neq \bar{2}$, $1 \neq 3$, $4 \neq 2$ and $4 \neq \bar{3}$ because the orbits breaking these rules have already been counted at $\mathcal{O}[\tau^2]$ of the expansion. For the same reason we insist that TR3b obeys $1 \neq \bar{1}$, $3 \neq \bar{3}$, $2 \neq \bar{4}$, while TR3c obeys $1 \neq \bar{1}$, $2 \neq \bar{2}$ and $3 \neq \bar{3}$. Note that some of the restrictions are superfluous since they refer to orbits that are already excluded. For example, we can drop the restriction $4 \neq \bar{3}$ because this is automatically enforced by the stronger restriction $s_3 \neq f_4$.

The complete set of restrictions is as follows:

- NTR3a: $\Delta_{\mathrm{NTR3a}} = \left(1 - \delta_{s_2 s_4}\right)\left(1 - \delta_{s_1 s_3}\right)$
- NTR3b: $\Delta_{\mathrm{NTR3b}} = \left(1 - \delta_{s_1 s_2}\right)\left(1 - \delta_{s_1 s_3}\right)\left(1 - \delta_{s_2 s_3}\right)$ where orbits with $(2, 3) = (\bar{2}, \bar{3})$ must be subtracted for systems with TR symmetry.
- TR3a: $\Delta_{\mathrm{TR3a}} = \left(1 - \delta_{s_2 s_4}\right)\left(1 - \delta_{s_3 f_4}\right)$ with $1 \neq \bar{2}$ and $1 \neq 3$.
- TR3b: $\Delta_{\mathrm{TR3b}} = \left(1 - \delta_{s_2 f_4}\right)\left(1 - \delta_{s_4 f_2}\right)$ with $1 \neq \bar{1}$ and $3 \neq \bar{3}$.
- TR3c: $\Delta_{\mathrm{TR3c}} = \left(1 - \delta_{s_2 s_3}\right)\left(1 - \tfrac{1}{2}\delta_{s_2 f_3}\right)\left(1 - \tfrac{1}{2}\delta_{s_1 f_2}\right)$ with $1 \neq \bar{1}$, $2 \neq \bar{2}$ and $3 \neq \bar{3}$.

We reiterate that this self-consistent set of restrictions is not unique. And, although this choice leads to simpler calculations than all the others we tried, we cannot rule out the possibility that there is another self-consistent set of restriction which would further simplify our calculations.

3.4. Orbit amplitudes

Before we can attempt the summation over all orbit pairs P, Q within a given diagram, we still need to understand the structure of the product $A_P A_Q^*$ appearing in equations (13), (16). We consider the diagram NTR3b as an example. Let arc 1 be of length t_1, consisting of the vertices $\left[x_1, x_2, \ldots, x_{t_1-1}\right]$, where $x_1 \equiv s_1$ and $x_{t_1-1} \equiv f_1$. Then both A_P and A_Q will contain factors $\sigma^{(x_1)}_{x_2,\alpha}, \sigma^{(x_2)}_{x_3,x_1}, \sigma^{(x_3)}_{x_4,x_2}, \ldots, \sigma^{(x_{t_1-1})}_{\alpha,x_{t_1-2}}$. Thus when we evaluate the product $A_P A_Q^*$, the contribution of the arc 1 will come in the form

$$\left|\sigma^{(x_1)}_{x_2,\alpha}\sigma^{(x_2)}_{x_3,x_1}\sigma^{(x_3)}_{x_4,x_2}\cdots\sigma^{(x_{t_1-1})}_{\alpha,x_{t_1-2}}\right|^2 = P_{(\alpha,x_1)\to(x_1,x_2)\to\cdots\to(x_{t_1-1},\alpha)} \equiv P_1 \tag{32}$$

which is the *classical* probability of following arc 1 from bond (α, s_1) to bond (f_1, α).[7] Analogous considerations for arcs 2 and 3 lead to the probabilities P_2 and P_3. The factors not yet accounted for in P_1, P_2, P_3 are the transition amplitudes picked up at the intersection vertex α:

$$A_P A_Q^* = P_1 \times P_2 \times P_3 \times \sigma^{(\alpha)}_{s_3 f_2}\sigma^{(\alpha)}_{s_2 f_1}\sigma^{(\alpha)}_{s_1 f_3} \times \left(\sigma^{(\alpha)}_{s_2 f_3}\sigma^{(\alpha)}_{s_3 f_1}\sigma^{(\alpha)}_{s_1 f_2}\right)^*. \tag{33}$$

To evaluate the contribution of a given diagram a product such as equation (33) must be summed over all free parameters, namely all intersection points and all possible arcs connecting these points. The latter summation includes a sum over the lengths t_i of these arcs with the restriction that the total length of the orbit is t.

The summation over all the intermediate vertices $x_2, x_3, \ldots, x_{t_1-2}$ along arc 1 can be performed immediately, because it is unaffected by the restrictions discussed in the previous subsection. This summation adds the classical probabilities of all possible paths leading from bond (α, s_1) to bond (f_1, α) in $t_1 - 1$ steps and results consequently in the classical transition probability $P^{(t_1-1)}_{(\alpha,s_1)\to(f_1,\alpha)}$ given by equation (7). Analogous summations over the other arcs produce $P^{(t_2-1)}_{(\alpha,s_2)\to(f_2,\alpha)}$ and $P^{(t_3-1)}_{(\alpha,s_3)\to(f_3,\alpha)}$. The above approach extends trivially to the TR diagrams when we recall that time-reversal symmetry implies that the matrices $\sigma^{(v)}$ are symmetric.

The remaining summation is over the lengths t_i of all arcs, the first and the last vertex s_i and f_i of all arcs i with $t_i > 1$ and the intersection points such as α. For general graphs this sum is still too complicated for explicit calculations, mainly because transition probabilities such as $P^{(t_1-1)}_{(\alpha,s_1)\to(f_1,\alpha)}$ are dependent on the details of the topology of the graph. For sufficiently long arcs, however, these transition probabilities can be replaced by B^{-1} according to equation (9). Then the sum over vertices decouples into a product of sums associated with each self-intersection vertex α which can finally be evaluated using the unitarity of the vertex-scattering matrices $\sigma^{(\alpha)}$. This is the strategy we shall follow in the next two sections, where explicit summation of the NTR3 and TR3 diagrams is performed.

4. Summing the NTR contributions

4.1. Summation of NTR3 diagrams

Starting with the NTR3a diagram, we write

$$K_{\mathrm{NTR3a}}(\tau) = \frac{1}{4}\frac{t^2}{B}\sum_{\{t_i\}}\delta\left[t - \sum_{i=1}^{4} t_i\right]\sum_{\alpha,\beta}\sum_{\{s_i,f_i\}}\Sigma_{\mathrm{NTR3a}} \times P_{\mathrm{NTR3a}} \times \Delta_{\mathrm{NTR3a}} \tag{34}$$

[7] $P_1 = 1$ if arc 1 contains no vertices, i.e. if $t_1 = 1$.

where

$$\Sigma_{\mathrm{NTR3a}} = \sigma^{(\alpha)}_{s_4 f_3}\sigma^{(\beta)}_{s_3 f_2}\sigma^{(\alpha)}_{s_2 f_1}\sigma^{(\beta)}_{s_1 f_4}\sigma^{(\alpha)*}_{s_2 f_3}\sigma^{(\beta)*}_{s_3 f_4}\sigma^{(\alpha)*}_{s_4 f_1}\sigma^{(\beta)*}_{s_1 f_2} \tag{35}$$

$$P_{\mathrm{NTR3a}} = P^{(t_1-1)}_{(\beta,s_1)\to(f_1,\alpha)}P^{(t_2-1)}_{(\alpha,s_2)\to(f_2,\beta)}P^{(t_3-1)}_{(\beta,s_3)\to(f_3,\alpha)}P^{(t_4-1)}_{(\alpha,s_4)\to(f_4,\beta)} \tag{36}$$

$$\Delta_{\mathrm{NTR3a}} = \big(1-\delta_{s_1 s_3}\big)\big(1-\delta_{s_2 s_4}\big). \tag{37}$$

As $t\to\infty$ and $t = t_1+t_2+t_3+t_4$, at least one of the arcs must be long. Without loss of generality we assume that $t_1 \geqslant t/4$. From equation (9) we have $P^{(t_1-1)}_{(\beta,s_1)\to(f_1,\alpha)} \approx B^{-1}$ and the only factors in equation (34) depending on f_1 are $\sigma^{(\alpha)}_{s_2 f_1}\sigma^{(\alpha)*}_{s_4 f_1}$. Using the unitarity of the σ-matrices we perform the summation

$$\sum_{f_1}\sigma^{(\alpha)}_{s_2 f_1}\sigma^{(\alpha)*}_{s_4 f_1} = \delta_{s_2 s_4}. \tag{38}$$

However, the restriction Δ_{NTR3a} contains the term $\big(1-\delta_{s_2 s_4}\big)$, leading to the result

$$K_{\mathrm{NTR3a}} = 0. \tag{39}$$

Calculation of K_{NTR3b} goes along the same route with

$$K_{\mathrm{NTR3b}}(\tau) = \frac{1}{3}\frac{t^2}{B}\sum_{\{t_i\}}\delta\left[t-\sum_{i=1}^{3}t_i\right]\sum_{\alpha}\sum_{\{s_i,f_i\}}\Sigma_{\mathrm{NTR3b}}\times P_{\mathrm{NTR3b}}\times\Delta_{\mathrm{NTR3b}} \tag{40}$$

where

$$\Sigma_{\mathrm{NTR3b}} = \sigma^{(\alpha)}_{s_3 f_2}\sigma^{(\alpha)}_{s_2 f_1}\sigma^{(\alpha)}_{s_1 f_3}\sigma^{(\alpha)*}_{s_2 f_3}\sigma^{(\alpha)*}_{s_3 f_1}\sigma^{(\alpha)*}_{s_1 f_2} \tag{41}$$

$$P_{\mathrm{NTR3b}} = P^{(t_1-1)}_{(\alpha,s_1)\to(f_1,\alpha)}P^{(t_2-1)}_{(\alpha,s_2)\to(f_2,\alpha)}P^{(t_3-1)}_{(\alpha,s_3)\to(f_3,\alpha)} \tag{42}$$

$$\Delta_{\mathrm{NTR3b}} = \big(1-\delta_{s_1 s_2}\big)\big(1-\delta_{s_2 s_3}\big)\big(1-\delta_{s_3 s_1}\big). \tag{43}$$

Exactly as for NT3a we can sum over f_i where arc i is long, which results in δ-function which we combine with Δ_{NTR3b} to get the answer

$$K_{\mathrm{NTR3b}} = 0. \tag{44}$$

The sum of the NTR3a and NTR3b diagrams vanishes and so

$$K_{\mathrm{NTR3}}(\tau) = 0. \tag{45}$$

Thus we see that for a wide class of quantum graphs without time-reversal symmetry the τ^3-contribution to the form factor is zero, as expected from the BGS conjecture.

We wish to note that the derivation given above is relatively simple, since NTR3a and NTR3b both vanish due to the particular choice of restrictions which make orbit pairs in the intersection of NTR3a and NTR3b unique (see the discussion near equation (25)). Had we chosen to assign all ambiguous diagrams to NTR3a, then the results for NTR3a and NTR3b would both have been non-zero, although the total sum $K_{\mathrm{NTR}}(\tau)$ would of course still have equalled zero.

To apply the above result to the TR case, described by (20), we must subtract the contribution of the NTR3b diagram with two self-retracing arcs, as discussed in section 3.3. We use the fact that long self-retracing arcs give only exponentially small corrections because the number of free summation variables is reduced by a factor of 2. Thus we only need to consider short self-retracing arcs. Without loss of generality we can assume that arcs 2 and 3 are self-retracing and short, implying that t_1 must be long enough for $P^{(t_1-1)} = B^{-1}$ to hold. Then the sum over f_1 results in a factor of $\delta_{s_2 s_3}$ and, combining this with the restriction Δ_{NTR3b}, we find that the contribution of this case is identically zero. Thus the NTR diagrams contribute nothing to the form factor of TR systems.

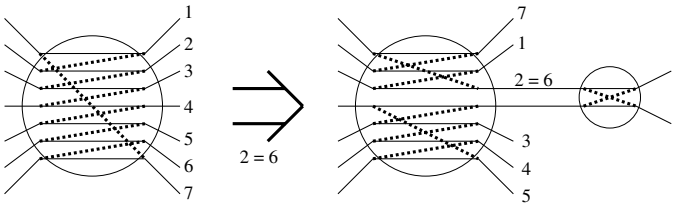

Figure 3. The picture on the left is a self-intersection in a NTR contribution with seven crossing arcs. If two bonds leaving this intersection coincide, in this case 2 and 6, the intersection can be redrawn (as on the right) as more than one intersection. In this case there are three intersections, one 2-intersection, one 3-intersection and one 4-intersection, the latter two being at the same vertex.

4.2. Generalization to higher orders

One may speculate that the arguments given in the previous subsection admit a straightforward generalization to higher-order diagrams. Given an nth-order diagram, we impose the following restriction on each of its intersections

$$\Delta = \prod_{i,j} \left(1 - \delta_{s_i s_j}\right) \tag{46}$$

where the product is over the set of all arcs leaving the intersection. Now we can evaluate diagrams in the same way as we did for $n = 3$. As soon as $n \ll t/t_{\mathrm{erg}}$ at least one arc must be long. If arc i is long then $P^{(t_i-1)} \simeq B^{-1}$ and the sum over f_i generates a δ-function. Combining this δ-function with the restriction at the vertex produces zero.

To justify the choice of the restriction (46) for any intersection, we note that if any two bonds leaving the vertex are the same, the intersection can be rearranged as a group of more than one intersection, each satisfying the above restriction. An example of such rearrangement is presented in figure 3. If the original intersection was part of an nth-order diagram, then the rearranged one is part of another valid nth-order diagram (as can be shown by counting the powers of B, see section 6). The above restriction thereby helps to prevent double counting of orbits with tangential intersections.

This argument essentially shows that the contribution of all nth-order diagrams is zero in the NTR case. However, an important detail is missing: one has to show that all eligible pairs of periodic orbits belong to *one and only one* diagram, i.e. that we did not miss anything and did not count anything more than once. Unfortunately we found pairs of orbits that violate both parts of this statement. These counterexamples seem to be 'rare', in the sense that the sum of their contributions vanish as $B \to \infty$, however a rigorous proof of this observation remains an open problem.

To summarize, a generalization of the argument of section 4.1 sketches a proof of exactness of the diagonal approximation for $\tau \leqslant 1$ in the absence of time-reversal symmetry. To complete the proof one would have to verify that the above restriction counts all relevant pairs of orbits once and only once.

5. Summation of TR3 diagrams for a fully connected 'Fourier' graph

Evaluating K_{TR3} for a general class of graphs is a complicated and tedious task [16]. Fortunately, the calculation simplifies considerably for a special case described below. In this section we restrict our attention to fully connected graphs with N vertices and $B = N^2$

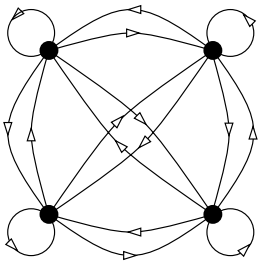

Figure 4. A fully connected graph with four vertices and sixteen directed bonds.

directed bonds, including a loop at each of the vertices. An example with $N = 4$ is shown in figure 4. We assume that the vertex-scattering matrices are

$$\sigma^{(l)}_{m'm} = \frac{1}{\sqrt{N}} \exp\left(2\pi \mathrm{i} \frac{mm'}{N}\right) \tag{47}$$

for all l. These matrices were proposed in [15] and result in a particularly fast convergence to RMT-like statistics. Because of the analogy to the discrete Fourier transformation from m to m', we call a vertex endowed with the scattering matrix (47) a 'Fourier' vertex. The corresponding matrix M represents uniform scattering at the vertex,

$$M_{m'l,lm} = \left|\sigma^{(l)}_{m'm}\right|^2 = N^{-1} \tag{48}$$

and thus the probability to get from (a, b) to (c, d) in t step is

$$P^{(t)}_{(a,b)\to(c,d)} = (M^t)_{(d,c),(b,a)} = \begin{cases} N^{-1}\delta_{bc} & t = 1 \\ B^{-1} & t > 1. \end{cases} \tag{49}$$

It is also useful to have an expression for $\widetilde{P}^{(t)}_{(a,b)\to(b,a)}$, the probability to get from (a, b) to (b, a) following only self-retracing paths. The contribution of each path is N^{-t} and, due to their special structure, a self-retracing path of $2m+1$ or $2m+2$ steps will contain m vertices not including the initial a and b. Each of these m vertices can be freely chosen from the N vertices of the graph, resulting in N^m different self-retracing paths. Thus, the probability $\widetilde{P}^{(t)}_{(a,b)\to(b,a)}$ takes the form

$$\widetilde{P}^{(t)}_{(a,b)\to(b,a)} = N^{-1-m} \qquad \text{with} \quad t = 2m \quad \text{or} \quad 2m+1 \tag{50}$$

i.e., it is indeed decaying exponentially in time.

5.1. Summation of TR3a

Here we calculate the contributions of orbits with the topology of TR3a which obey the conditions $s_2 \neq s_4$ and $s_3 \neq f_4$. We enforce these conditions by multiplying the contribution of all orbits of this topology by

$$\Delta_{\mathrm{TR3a}} = \left(1 - \delta_{s_2 s_4}\right)\left(1 - \delta_{s_3 f_4}\right). \tag{51}$$

Thus the contribution of TR3a is

$$K_{\mathrm{TR3a}}(\tau) = \frac{1}{2}\frac{t^2}{B} \sum_{\{t_i\}} \delta\left[t - \sum_{i=1}^{4} t_i\right] \sum_{\alpha,\beta} \sum_{s_i, f_i} \Sigma_{\mathrm{TR3a}} \times P_{\mathrm{TR3a}} \times \Delta_{\mathrm{TR3a}} \tag{52}$$

where

$$\Sigma_{\mathrm{TR3a}} = \sigma^{(\alpha)}_{s_4 f_3}\sigma^{(\beta)}_{s_3 f_2}\sigma^{(\alpha)}_{s_2 f_1}\sigma^{(\beta)}_{s_1 f_4}\sigma^{(\alpha)*}_{f_3 s_2}\sigma^{(\beta)*}_{f_2 f_4}\sigma^{(\alpha)*}_{s_4 f_1}\sigma^{(\beta)*}_{s_1 s_3} \tag{53}$$

$$P_{\mathrm{TR3a}} = P^{(t_1-1)}_{(\beta,s_1)\to(f_1,\alpha)}P^{(t_2-1)}_{(\alpha,s_2)\to(f_2,\beta)}P^{(t_3-1)}_{(\beta,s_3)\to(f_3,\alpha)}P^{(t_4-1)}_{(\alpha,s_4)\to(f_4,\beta)}. \tag{54}$$

If arc 1 is long enough to be ergodic, the sum over s_1 simplifies to

$$\bigl(1-\delta_{s_3 f_4}\bigr)\sum_{s_1}\sigma^{(\beta)}_{s_1 f_4}\sigma^{(\beta)*}_{s_1 s_3} = \bigl(1-\delta_{s_3 f_4}\bigr)\delta_{s_3 f_4} = 0. \tag{55}$$

If arc 2 or arc 3 is ergodic we can carry out a similar sum over f_2 or f_3 respectively, these sums also yield the answer zero. Thus we can only get a non-zero contribution when arc 4 is the only ergodic path. However, we argue in section 6 that we need at least two arcs to be long (ergodic) since otherwise the contribution can be neglected. Thus the non-zero contribution discussed above will only give a small correction which will vanish in the limit $B\to\infty$. The two restrictions $1\neq\bar{2}$ and $1\neq 3$ do not change the above argument at all, so we have ignored them. We conclude that

$$K_{\mathrm{TR3a}}(\tau) = 0. \tag{56}$$

5.2. Summation of TR3b

Here we calculate the contributions of orbits with the topology of TR3b which obey the conditions $s_2\neq f_4$, $s_4\neq f_2$, $1\neq\bar{1}$ and $3\neq\bar{3}$. The first two conditions will be enforced by means of a factor

$$\Delta_{\mathrm{TR3b}} = \bigl(1-\delta_{s_2 f_4}\bigr)\bigl(1-\delta_{s_4 f_2}\bigr). \tag{57}$$

The latter two we will enforce below 'by hand'. Thus

$$K_{\mathrm{TR3b}}(\tau) = \frac{1}{2}\frac{t^2}{B}\sum_{\{t_i\}}\delta\left[t-\sum_{i=1}^{4}t_i\right]\sum_{\alpha,\beta}\sum_{s_i,f_i}\Sigma_{\mathrm{TR3b}}\times P_{\mathrm{TR3b}}\times\Delta_{\mathrm{TR3b}} \tag{58}$$

where

$$\Sigma_{\mathrm{TR3b}} = \sigma^{(\beta)}_{s_4 f_3}\sigma^{(\beta)}_{s_3 f_2}\sigma^{(\alpha)}_{s_2 f_1}\sigma^{(\alpha)}_{s_1 f_4}\sigma^{(\beta)*}_{f_2 f_3}\sigma^{(\beta)*}_{s_3 s_4}\sigma^{(\alpha)*}_{f_4 f_1}\sigma^{(\alpha)*}_{s_1 s_2} \tag{59}$$

$$P_{\mathrm{TR3b}} = P^{(t_1-1)}_{(\alpha,s_1)\to(f_1,\alpha)}P^{(t_2-1)}_{(\alpha,s_2)\to(f_2,\beta)}P^{(t_3-1)}_{(\beta,s_3)\to(f_3,\beta)}P^{(t_4-1)}_{(\beta,s_4)\to(f_4,\alpha)}. \tag{60}$$

We only need to consider cases where $t_1\geqslant 3$ and $t_3\geqslant 3$ because shorter arcs are purely self-retracing ($1=\bar{1}$) and so must be excluded. We will treat the restrictions $1\neq\bar{1}$ and $3\neq\bar{3}$ using the following inclusion–exclusion procedure: the sum in (58) with these restrictions is equal to the sum without the restrictions, minus the sum with $1=\bar{1}$, minus the sum with $3=\bar{3}$, plus the sum with both $1=\bar{1}$ and $3=\bar{3}$.

The first sum yields zero after the summation over s_1 or over s_3 in a fashion similar to equation (55). The second sum we perform with respect to s_3 while the third is summed with respect to s_1, in both cases the answer is zero. Thus $K_{\mathrm{TR3b}}(\tau)$ is equal to the sum with both $1=\bar{1}$ and $3=\bar{3}$, which can be written as

$$K_{\mathrm{TR3b}}(\tau) = \frac{1}{2}\frac{t^2}{B^3}\sum_{\{t_i\}}\delta\left[t-\sum_{i=1}^{4}t_i\right] \times\sum_{\alpha,\beta}\sum_{s_i,f_i}\widetilde{P}^{(t_1-1)}_{(\alpha,s_1)\to(s_1,\alpha)}\widetilde{P}^{(t_3-1)}_{(\beta,s_3)\to(s_3,\beta)}\times\Delta_{\mathrm{TR3b}}\times\Sigma_{\mathrm{TR3b}}\times\delta_{s_1,f_1}\delta_{s_3,f_3} \tag{61}$$

where we used the fact that $P^{(t_j-1)}_{(\alpha,s_j)\to(f_j,\beta)} = B^{-1}$ for $j = 2, 4$, while $\tilde{P}^{(t)}_{(a,b)\to(b,a)}$ is defined above equation (50). Upon substitutions $f_1 = s_1$ and $f_3 = s_3$, and using the symmetry of the matrices σ, equation (14), Σ_{TR3b} becomes

$$\Sigma_{\mathrm{TR3b}} = \left|\sigma^{(\alpha)}_{s_1 f_4}\right|^2 \left|\sigma^{(\alpha)}_{s_2 s_1}\right|^2 \left|\sigma^{(\beta)}_{s_3 f_2}\right|^2 \left|\sigma^{(\beta)}_{s_4 s_3}\right|^2 = N^{-4}. \tag{62}$$

We also note that the probabilities $\widetilde{P}$ do not depend on the start and end bonds. Now we can perform the sum over α, β and all s_i and f_i, which, taking into account various delta-functions, gives the factor $N^6(N-1)^2$. We get

$$K_{\mathrm{TR3b}}(\tau) = \frac{1}{2}\frac{t^2N^2(N-1)^2}{B^3}\sum_{\{t_i\}}\delta\left[t - \sum_{i=1}^{4} t_i\right]\widetilde{P}^{(t_1-1)}\widetilde{P}^{(t_3-1)} \tag{63}$$

from which it is clear that the dominant contribution comes from $t_1 = 3$ or 4 and $t_3 = 3$ or 4; the contributions from other values of t_1 and t_3 are of order $O(N^{-1})$. After carrying out the sum over t_2 using the δ-function which forces $t_4 = t - t_2 - n$ with $n = t_1 + t_3 = 6, 7, 8$ we get

$$K_{\mathrm{TR3b}} = 4 \times \frac{1}{2}\frac{t^2}{B^3}\sum_{t_2=3}^{t-3-n} 1 = 2\frac{t^3}{B^3} = 2\tau^3 \tag{64}$$

where we have dropped corrections which vanish in the limit $B, N \to \infty$ and the factor 4 comes from the number of possible choices of t_1 and t_3.

5.3. Summation of TR3c

Here we calculate the contributions of orbits with the topology of TR3c which obey the following restrictions. First we should only count *half* the contribution when $s_2 = f_3$ or $s_1 = f_2$. Secondly $s_2 \neq s_3$, $1 \neq \bar{1}$, $2 \neq \bar{2}$ and $3 \neq \bar{3}$. The restrictions which apply to whole arcs will again be enforced 'by hand' using an inclusion–exclusion procedure similar to that used above, the rest of the restrictions are

$$\Delta_{\mathrm{TR3c}} = \left(1 - \delta_{s_2 s_3}\right)\left(1 - \tfrac{1}{2}\delta_{s_2 f_3}\right)\left(1 - \tfrac{1}{2}\delta_{s_1 f_2}\right). \tag{65}$$

Thus

$$K_{\mathrm{TR3c}}(\tau) = \frac{t^2}{B}\sum_{\{t_i\}}\delta\left[t - \sum_{i=1}^{3} t_i\right]\sum_{\alpha}\sum_{s_i, f_i}\Sigma_{\mathrm{TR3c}} \times P_{\mathrm{TR3c}} \times \Delta_{\mathrm{TR3c}} \tag{66}$$

where

$$\Sigma_{\mathrm{TR3c}} = \sigma^{(\alpha)}_{s_3 f_2}\sigma^{(\alpha)}_{s_2 f_1}\sigma^{(\alpha)}_{s_1 f_3}\sigma^{(\alpha)*}_{f_2 f_3}\sigma^{(\alpha)*}_{s_3 f_1}\sigma^{(\alpha)*}_{s_1 s_2} \tag{67}$$

$$P_{\mathrm{TR3c}} = P^{(t_1-1)}_{(\alpha,s_1)\to(f_1,\alpha)}P^{(t_2-1)}_{(\alpha,s_2)\to(f_2,\alpha)}P^{(t_3-1)}_{(\alpha,s_3)\to(f_3,\alpha)}. \tag{68}$$

The summation here is similar to the sums in TR3b: first we ignore the restriction $1 \neq \bar{1}$ (but enforce the restrictions $2 \neq \bar{2}$ and $3 \neq \bar{3}$) and carry out the sum over f_1 to get

$$\left(1 - \delta_{s_2 s_3}\right)\sum_{f_1}\sigma^{(\alpha)}_{s_2 f_1}\sigma^{(\alpha)*}_{s_3 f_1} = \left(1 - \delta_{s_2 s_3}\right)\delta_{s_2 s_3} = 0. \tag{69}$$

Then we subtract the sum over orbits with $1 = \bar{1}$ (again enforcing the restrictions $2 \neq \bar{2}$ and $3 \neq \bar{3}$). Similar to TR3b, it turns out that the dominant contribution comes from orbits with

$t_1 = 3, 4$, i.e. $\widetilde{P}^{(t_1-1)} = N^{-2}$. Since $t_1 \ll t$ we use the argument from section 6 to note that we are only interested in orbits where $t_2, t_3 \sim t$ and thus both arcs 2 and 3 are ergodic. This leaves us with

$$K_{\mathrm{TR3c}}(\tau) = -2 \times \frac{t^2}{B^3 N^2} \sum_{t_2+t_3=t-n} \sum_{\alpha} \sum_{s_i, f_i} \Sigma_{\mathrm{TR3c}} \times \Delta_{\mathrm{TR3c}} \times \delta_{s_1, f_1} \tag{70}$$

where $n = 3, 4$. We sum over f_1 using equation (14) to get

$$\Sigma_{\mathrm{TR3c}} = \left|\sigma^{(\alpha)}_{s_2 s_1}\right|^2 \sigma^{(\alpha)}_{s_1 f_3} \sigma^{(\alpha)}_{s_3 f_2} \sigma^{(\alpha)*}_{f_2 f_3} \sigma^{(\alpha)*}_{s_3 s_1} = N^{-1} \sigma^{(\alpha)}_{s_1 f_3} \sigma^{(\alpha)}_{s_3 f_2} \sigma^{(\alpha)*}_{f_2 f_3} \sigma^{(\alpha)*}_{s_3 s_1} \tag{71}$$

open up the brackets in Δ_{TR3c},

$$\left(1 - \tfrac{1}{2}\delta_{s_2 f_3}\right)\left(1 - \tfrac{1}{2}\delta_{s_1 f_2}\right) = \left(1 - \tfrac{1}{2}\delta_{s_1 f_2}\right) - \tfrac{1}{2}\delta_{s_2 f_3} + \tfrac{1}{4}\delta_{s_2 f_3}\delta_{s_1 f_2} \tag{72}$$

and are now facing the sum

$$\sum_{\alpha, s_1, s_2, f_2, s_3, f_3} \sigma^{(\alpha)}_{s_1 f_3} \sigma^{(\alpha)}_{s_3 f_2} \sigma^{(\alpha)*}_{f_2 f_3} \sigma^{(\alpha)*}_{s_3 s_1} \left(1 - \delta_{s_2 s_3}\right) \left[\left(1 - \frac{1}{2}\delta_{s_1 f_2}\right) - \frac{1}{2}\delta_{s_2 f_3} + \frac{1}{4}\delta_{s_2 f_3}\delta_{s_1 f_2}\right]. \tag{73}$$

Invoking the unitarity of the σ-matrices, it is an easy exercise to show that this sum evaluates to $N^2(N-1)/2 + N(N-1)/4$.

Combining the above information and ignoring subdominant contributions we arrive at

$$K_{\mathrm{TR3c}}(\tau) = -2\frac{t^2}{B^3 N^3} \sum_{t_2} N^2(N-1)/2 = -\tau^3. \tag{74}$$

5.4. The TR3 result

Remembering that we proved $(K_{\mathrm{NTR3a}} + K_{\mathrm{NTR3b}}) = 0$ in section 4.1, we simply need to substitute the results of the three previous subsections into equation (20) to get

$$K_{\mathrm{TR3}}(\tau) = 2\tau^3. \tag{75}$$

Combining this result with the one in [10] *proves* that the form factor for the fully connected Fourier graph coincides with the GOE form factor up to the third order in τ.

6. Estimating the order of a diagram

In this section, we discuss a rule for finding all diagrams which contribute to the nth order in the small τ expansion of the form factor. The rule is

$$(\text{number of arcs}) - (\text{number of intersections}) = (n-1). \tag{76}$$

Thus for $n = 2$, we need only one diagram which is (2, 1) in the format (number of arcs, number of intersections), and this is the contribution we considered in [10]. Here we are interested in $n = 3$, so we must consider both (3, 1) and (4, 2). It is these diagrams that we show in figure 1.

To get the rule (76) we count powers of B in a diagram's contribution. Equations (13) and (16) have a prefactor of B^{-1} so a τ^n-contribution to the form factor must get $B^{-(n-1)}$ from the summation over the orbits. In the ergodic limit, according to equation (9), each arc will contribute the weight B^{-1}, while each intersection contributes the weight B, thus we have equation (76). The origin of the factor of B associated with each intersection can be explained as follows. First of all, the set of all vertices $\{v_j\}$ adjacent to an intersection point

γ can be split into two equal subsets satisfying the following property: if there is a transition $(v_j, \gamma) \to (\gamma, v_m)$ in either P or Q then v_j and v_m belong to different subsets[8]. This is particularly simple for the NTR3 diagrams where the two sets are simply $\{s_i\}$ and $\{f_i\}$. If we now do the summation over all vertices in one subset and invoke the unitarity of the scattering matrix at the vertex γ, the result will be a product of δ-functions $\delta_{u_1u_2}\delta_{u_2u_3}\cdots\delta_{u_ku_1}$ where u_k are the vertices from the second subset, ordered in an appropriate way. Now the summation over $u_2, \ldots, u_k$ will give 1 while the summation over u_1 and γ will give the sought-after factor of B, since the only restriction on u_1 and γ is that they have to be the two ends of the same bond.

To make this recipe work for the diagonal term ($\sim\tau^1$), the corresponding diagram being just a looping arc, we need one extra ingredient, the starting vertex for the loop. The position of the vertex is not determined, it can be placed anywhere on the looping arc, unlike the intersection points in other diagrams. To compensate for this ambiguity when we sum over all periodic orbits fitting such diagram, we divide the sum by the number of vertices in the loop, t.

Now we discuss why counting of powers of t does *not* work for obtaining equation (76). Let us estimate the order of t for a given diagram. Firstly, there is t^2 in the prefactor of equation (13) or (16). Secondly, for a diagram with a arcs, the lengths t_i of arcs satisfy $\sum_i t_i = t$ thus the sum over all possible t_i gives a factor proportional to t^{a-1}. Then of the diagrams in figure 1, NTR3b and TR3c appear to have four powers of t while the rest have five. Similarly, the diagram we evaluated in [10] gets three powers of t. The leading contributions to all the diagrams appear to have at least one more power of t than they should[9]. However, we show in [10] and the present paper that the numerical coefficient of this 'out of order' term is zero—at least for diagrams contributing up to third order in τ.

The arguments given above in favour of equation (76) are certainly too vague to be considered a proof. In particular, we cannot presently check our assumption that terms giving incorrectly large powers in t disappear also for more complicated diagrams. However, summing rigorously the contributions of all the diagrams obtained from this set of rules we show *a posteriori* that we indeed get an expansion which depends only on the scaled time τ. We also take confidence in our method from the fact that our rule generates the same diagrams that were used in perturbative calculations of the form factor for disordered systems with the nonlinear sigma model [12].

Nevertheless, counting powers of t is very useful in the following situation: if for some reason the lengths of some arcs are forced to be fixed, the estimated power of t can drop low enough that we can safely ignore the contribution of such a diagram in the $B \to \infty$ limit without actually evaluating it. In particular, we see that to get a non-vanishing contribution of order τ^3, at least two arcs in any diagram must have unrestricted lengths. Note that this does *not* mean that there is no contribution from orbit pairs where the maximum length of all arcs is restricted. For any given B and t there are orbit pairs with so many self-intersections that the maximum arc length is less than the time required for ergodicity. Then the method discussed in this paper must fail, this may explain why the power series expansion in τ breaks down at $\tau = 1$ for NTR (and at $\tau = 1/2$ for TR) despite the fact that the PO sums equations (13), (16) are exact.

[8] In other words the graph built on vertices v_j, connected if there is a transition $(v_j, \gamma) \to (\gamma, v_m)$, is bipartite. This graph is nothing else but the structure drawn inside the circles in figure 1. The graph is bipartite since it is 2-regular (the valency of each vertex is 2) and each connected component contains an even number of bonds.

[9] This, however, is not the case for the 'diagonal' diagram where the power of t is right, which explains why advancing beyond the diagonal approximation was (and still is) so hard.

7. Conclusions

At first sight, the achievements of the present paper may appear moderate. What is the point in going from second to third order in a series which is infinite, in particular if this step becomes possible only by restricting the range of systems considered to very special models? But we believe that such a point of view is too short-sighted. Semiclassical theories are obviously indispensable for a complete understanding of spectral statistics in systems with chaotic classical dynamics. As they are not based on a random matrix conjecture, such theories have the potential to account for important system-specific corrections which one can hope to extract once the emergence of universality within semiclassics is fully understood. On the other hand, the restriction to the diagonal approximation has so far severely limited the success of the semiclassical approach.

Going beyond the diagonal approximation in semiclassical PO theories is possible, as demonstrated by Sieber and Richter [1, 2]. But when more than a first-order correction is required, one will inevitably encounter the problems discussed in this paper. For example, one needs methods to select diagrams contributing at a given order, and we suggested a solution in section 6. It will be necessary to account for the ambiguity introduced by the representation of the form factor in terms of diagrams, and we have solved this problem at least in quantum graphs for the diagrams which contribute up to third order (section 3.3). It is important to note that a variety of orbits give the relevant contributions, and our calculations in section 5 indicate that the generalization of the leading-order correction to higher orders cannot be achieved by considering a single type of diagram only.

Here the third-order result for TR systems is limited to a class of uniformly hyperbolic quantum graphs. However, we have no reason to believe that any conclusion will be substantially changed when the calculation is done for a more generic model as, e.g., in [16]. While going further than third order for TR systems is beyond us at the moment, the prospects for doing this in NTR systems are more promising. We hope that the method presented in section 4.2 will prove applicable there.

Acknowledgments

We gratefully acknowledge extremely productive discussions held with M Sieber and U Smilansky. We also would like to thank the group of Professor F Haake in Universität Essen for hospitality and exchange of ideas. We are grateful to a referee who found a large number of misprints and inconsistencies in the paper and helped us improve the presentation of section 3.2. A significant part of the research was performed while both GB and RW were working at the Weizmann Institute of Science, Rehovot, Israel. During that time GB was supported by the Israel Science Foundation, a Minerva grant and the Minerva Center for Nonlinear Physics; and RW was supported by the US–Israel Binational Science Foundation (BSF) and the German–Israel Foundation (GIF). HS thanks the Weizmann Institute for kind hospitality during a number of visits. RW is now supported by an EPSRC grant.

References

[1] Sieber M and Richter K 2001 *Phys. Scr.* T **90** 128
[2] Sieber M 2002 *J. Phys. A: Math. Gen.* **35** 613
[3] Bohigas O, Giannoni M J and Schmit C 1984 *Phys. Rev. Lett.* **52** 1–4
[4] Haake F 2000 *Quantum Signatures of Chaos* (Berlin: Springer)
[5] Mehta M L 1991 *Random Matrices* (Boston: Academic)
[6] Gutzwiller M C 1971 *J. Math. Phys.* **12** 343–58

[7] Berry M V 1985 *Proc. R. Soc.* A **400** 229–51
[8] Kottos T and Smilansky U 1997 *Phys. Rev. Lett.* **79** 4794–7
[9] Kottos T and Smilansky U 1999 *Ann. Phys., NY* **274** 76–124
[10] Berkolaiko G, Schanz H and Whitney R S 2002 *Phys. Rev. Lett.* **88** 104101
[11] Braun P A, Haake F and Heusler S 2002 *J. Phys. A: Math. Gen.* **35** 1381
[12] Smith R A, Lerner I V and Altshuler B L 1998 *Phys. Rev.* B **58** 10343
[13] Barra F and Gaspard P 2000 *J. Stat. Phys.* **101** 283–319
[14] Norris J R 1997 *Markov Chains* (Cambridge: Cambridge University Press)
[15] Tanner G 2001 *J. Phys. A: Math. Gen.* **34** 8485
[16] Berkolaiko G 2003 *Preprint* nlin.CD/0305009